Mechanically and optically reliable folding structure with a hyperelastic material for seamless foldable displays

Hyuk-Jun Kwon, HongShik Shim, Sunkook Kim, Woong Choi, Youngtea Chun, InSeo Kee, and SangYoon Lee

Citation: Applied Physics Letters **98**, 151904 (2011); doi: 10.1063/1.3576906
View online: http://dx.doi.org/10.1063/1.3576906
View Table of Contents: http://scitation.aip.org/content/aip/journal/apl/98/15?ver=pdfcov
Published by the AIP Publishing

Mechanically and optically reliable folding structure with a hyperelastic material for seamless foldable displays

Hyuk-Jun Kwon,[a] HongShik Shim, Sunkook Kim, Woong Choi, Youngtea Chun, InSeo Kee, and SangYoon Lee[b]
Samsung Advanced Institute of Technology, Mt. 14-1, Nongseo-dong, Giheung-gu, Yongin-Si, Gyeonggi-do, Republic of Korea

(Received 21 February 2011; accepted 13 March 2011; published online 11 April 2011)

We report a mechanically and optically robust folding structure to realize a foldable active matrix organic-light-emitting-diode (AMOLED) display without a visible crease at the junction. A nonlinear stress analysis, based on a finite element method, provided an optimized design. The folding-unfolding test on the structure exhibited negligible deterioration of the relative brightness at the junction of the individual panels up to 10^5 cycles at a folding radius of 1 mm, indicating highly reliable mechanical and optical tolerances. These results demonstrate the feasibility of seamless foldable AMOLED displays, with potentially important technical implications on fabricating large size flexible displays. © *2011 American Institute of Physics*. [doi:10.1063/1.3576906]

There has been a great interest in a flexible, extendable flat panel display, since it can allow a large screen, a small form factor, and an easy portability. Although significant progress has been made in achieving a rollable or a flexible organic-light-emitting-diode (OLED) display, it is still a challenge to realize such a display at a small folding radius under 5 mm.[1] One of the approaches, suggested to overcome the limitation and to further provide a larger screen size, is to develop a display composed of multiple glass panels, such as dual displays[2] or tiled displays.[3,4] However, in spite of the extended screen size, these display devices possess a major drawback—a visible crease of the folding structure between individual panels.[5] Because the folding structure commonly consists of a hyperelastic material interfacing glass panels, removal of the visible crease of the folding structure requires a hyperelastic material that has (i) a matching refractive index to that of a glass panel to suppress the total reflection at the junction and (ii) a mechanical reliability up to a certain level of folding-unfolding cycles.

Hyperelastic materials are commonly used for flexible and large deformed applications.[6–9] Among hyperelastic materials that can be potentially used in the folding structure, silicone rubbers show promising properties: their maximum elongations are in the range of 100%–1100% and their refractive indexes are ~1.4, which are very close to that of a glass panel (1.51). In this study, we therefore, investigate the mechanically and optically stable folding structure composed of the silicone rubber to demonstrate the feasibility of fabricating a seamless foldable active matrix OLED (AMOLED) display. We first design an optimized folding structure based on a nonlinear finite element method (FEM) analysis with ABAQUS (produced by Dassault Systèmes), and then test its mechanical and optical tolerances by measuring the relative brightness at the junction up to 10^5 cycles of folding-unfolding at a folding radius of 1 mm.

Figure 1(a) shows a prototype seamless foldable AMOLED display, along with a schematic view of a folding window module attached to two AMOLED panels. The fabrication process and structure of the proof of concept for the foldable display was briefly described in our previous publication.[10] The folding window module includes a protective cover glass (GorillaTM Glass), two AMOLED display panels (panels 1 and 2), and a hyperelastic material. The protective cover glass not only prevents mechanical scratches but also provides a touch screen function. This folding structure enabled the foldable display to be folded by 180° as shown in Fig. 1(b).

To display an image as shown in Fig. 2(a), the AMOLED display panels need to be placed in a hyperelastic material of which refractive index matches to that of a glass panel. By the definition of total internal reflection, incident light is totally reflected off the surface if the angle of incidence is greater than the critical angle θ_c, which is given by Snell's law as follows:

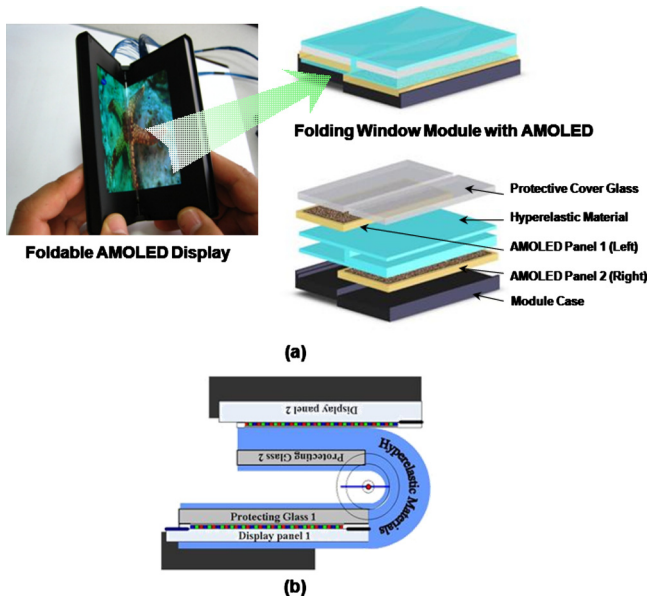

FIG. 1. (Color online) Schematic view of (a) the structure of the folding window module for proposed foldable AMOLED display and (b) the fully folded state of the folding window module at 180°.

[a]Electronic mail: www.hyukjun.kwon@gmail.com.
[b]Author to whom correspondence should be addressed. Electronic mail: sangyoon.lee@samsung.com.

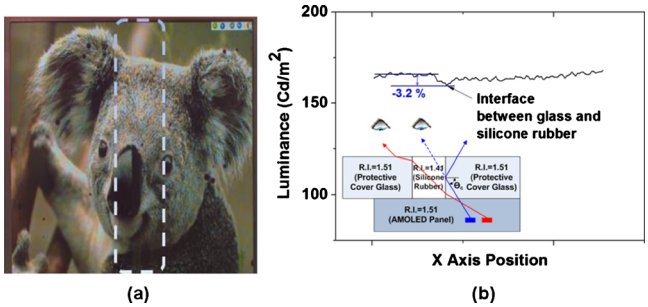

FIG. 2. (Color online) (a) Photographic images on the screen of prototype foldable AMOLED display without visible crease and (b) the change in luminance at the interface between a glass and a silicone rubber.

$$\theta_c = \sin^{-1}\left(\frac{n_2}{n_1}\right), \tag{1}$$

where n_2 and n_1 are the refractive indexes of the hyperelastic material and the glass, respectively. As the ratio of n_2/n_1 approaches 1 (i.e., θ_c approaches 90°), less light is reflected off the interface, implying that the crease will be less visible. With a silicon rubber (LSR 7060 produced by Momentive Performance Materials Inc.), of which refractive index (1.41) is very close to that of the glass panel (1.51), we observed a falling-off in luminance by up to 3.2% as shown in Fig. 2(b). However, the variation in luminance by this degree would be below the level that human eyes can recognize.

Stress-strain curve of the silicone rubber, measured with a standard tensometer, is shown in Fig. 3(a) in the overall strain range. Ultimate tensile stress of 5.69 MPa was obtained at the maximum elongation of 386%. In general, the stress-strain curve of elastomers depends on the maximum loading previously encountered. Commonly referred as Mullins effect,[11] instantaneous and irreversible softening of the stress-strain curve occurs whenever the load increases beyond its prior all-time maximum value. To check the Mullins effect in our system, stress-strain curves were obtained with cyclic loading/unloading uniaxial and biaxial tensile tests, as illustrated in Figs. 3(b) and 3(c). In this test, the silicone rubber was strained by 25% repeatedly for ten times before it was further strained by 50% for ten times. Note that the biaxial tensile extension creates a state of strain equivalent to that of a pure compression. As a result, in Figs. 3(b) and 3(c), only negligible decreases in stress softening in the stress-strain curves can be observed in both uniaxial and biaxial tensile tests (~3.7% and ~3.0%, respectively).

To understand and predict the behavior of the material, we use strain energy potential, $U(\varepsilon)$, which defines the strain energy stored in the material per unit volume with respect to the strain at that point in the material. Among a large variety of stain energy potentials that have been presented to model hyperelastic materials, Ogden model is a good match for both uniaxial and biaxial test data within the needed strain range ($\leq$1.0). The Ogden strain energy potential, expressed in terms of the principle stretches, can be given by:

$$U = \sum_{i=1}^{N} \frac{2\mu_i}{\alpha_i^2}\left(\bar{\lambda}_1^{\alpha i} + \bar{\lambda}_2^{\alpha i} + \bar{\lambda}_3^{\alpha i} - 3\right) + \sum_{i=1}^{N} \frac{1}{D_i}(J_{el} - 1)^{2i}, \tag{2}$$

where $\bar{\lambda}_i$ are the deviatoric principal stretches ($\bar{\lambda}_i = J^{-1/3}\lambda_i$); λ_i are the principal stretches; μ_i, α_i and D_i are material parameters. In addition, the elastic volume ratio, J_{el}, is given by $J_{el} = J/J_{th}$, where J is the total volume strain and J_{th} is the thermal volume strain. Assuming an axis-symmetry structure with an incompressible (D_i are ignored), isotropic, and large deformed nonlinear process provides $J = \det(F) = 1$ and $\lambda_1\lambda_2\lambda_3 = 1$, where F is a deformation gradient, expressed in the principal directions of stretch, given by:

$$F = \begin{bmatrix} \lambda_1 & 0 & 0 \\ 0 & \lambda_2 & 0 \\ 0 & 0 & \lambda_3 \end{bmatrix}. \tag{3}$$

The initial shear modulus and bulk modulus are given by $\mu_0 = \sum_{i=1}^{N} \mu_i$ and $K_0 = 2/D_1$, respectively.

The result of an FEM analysis with ABAQUS on a half of the symmetric folding structure is shown in Fig. 4(a). With the results of uniaxial and biaxial tensile tests put into the model, the Ogden strain energy potential [Eq. (2)] can predict the behavior of the folding structure, focused on the outmost and the inmost areas of the silicone rubber [point (1) and (2), respectively] and the outside edge of the interface between the silicone rubber and the glass [point (3)]. FEM analysis was carried out with changing the thickness of the glass (t) and the gap between the silicone rubber and the glass (L) in Fig. 4(a). Through the FEM computational result, internal forces such as tensile, compressive, and shear forces were obtained with respect to the external folding force. Figure 4(b) shows that the silicone rubber in the folding structure can endure at the given conditions (0.5 mm $\leq t \leq$ 1.0 mm and 3 mm $\leq L \leq$ 5 mm) because the gener-

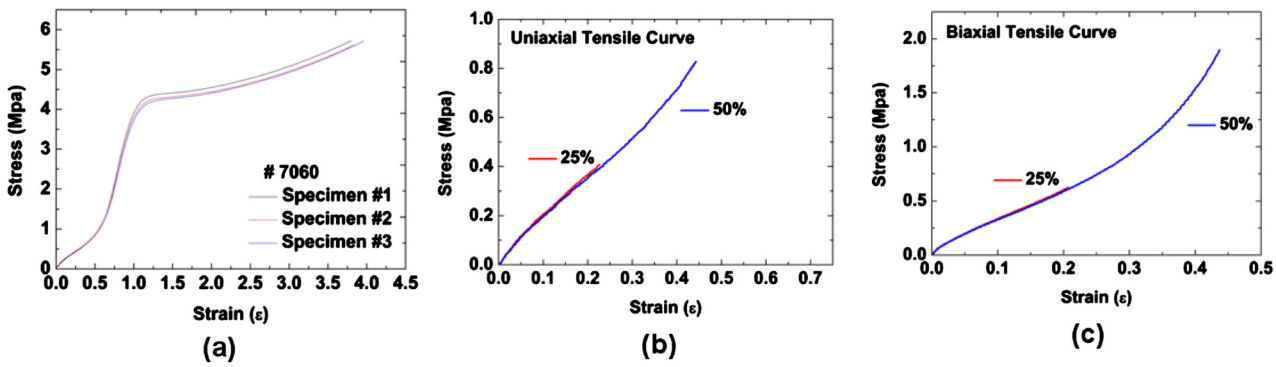

FIG. 3. (Color online) (a) Uniaxial tensile stress-strain curve of the hyperelastic material (LSR 7060) in the whole strain range; (b) cyclic uniaxial tensile stress-strain curve; and (c) cyclic biaxial tensile stress-strain curve for the strains of 25% and 50%.

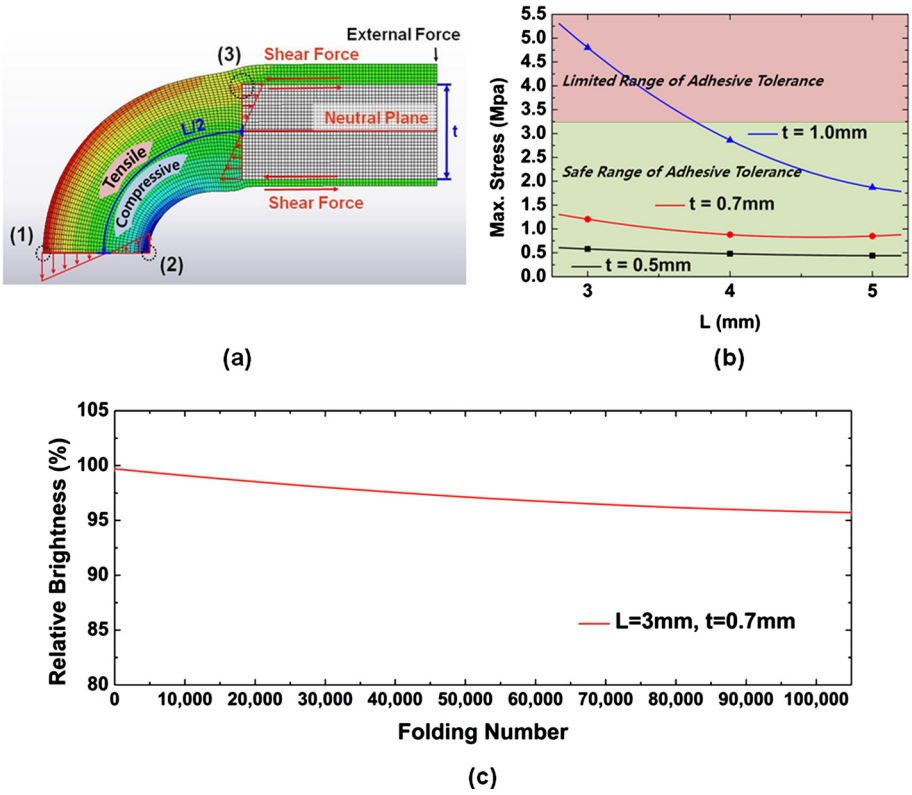

FIG. 4. (Color online) (a) FEM model design of a half of the folding window module at the final state after folding at 90° and (b) the results of FEM analysis and range of adhesive tolerance with respect to occurred stress at the folding window module; (c) the change in the relative brightness during 10^5 cycles of folding-unfolding test with L (3 mm) and t (0.7 mm) in the green region in (b).

ated maximum stress in the material is under the destructive stress and elongation (5.69 MPa and 386%, respectively). In addition, we observed adhesive tolerance between the hyperelastic material and the rigid body at point (3) to exist in the range between 3.3 and 4.4 MPa. Hence, to obtain a robust low-stress structure, the generated stress should be below both the maximum stress in the hyperelastic material and the adhesion stress of the interface [green region in Fig. 4(b)]. Since the reduced distance from the neutral plane lowers the stress at points (1), (2), and (3) in Fig. 4(a), it is understandable that thinner t and wider L generate lower stress in Fig. 4(b). However, if t becomes too thin, the display becomes vulnerable to external impact. (For this reason, commercial products with a large built-in screen typically come equipped with a toughened glass with its thickness of 0.7 mm.) On the other hand, when L becomes too wide, it is hard to connect the touch screen function embedded on two individual glasses by software. It also increases the whole thickness of the display device due to the increased folding radius.

To confirm the results from the simulation, mechanical and the optical tolerances against folding was measured for different structural dimensions of L and t. With a SPECTRASCAN Colorimeter (Photo Research, Inc.), relative brightness of the folded structure with respect to its initial value was measured for every 10^4 cycles of folding-unfolding test at a folding radius of 1mm. When L was 2 mm wide, the interface was destroyed within only a few folding-unfolding cycles, indicating that the generated internal stress was beyond the adhesion tolerance. However, as shown in Fig. 4(c), with L (3 mm) and t (0.7 mm) in the green region in Fig. 4(b), the relative brightness decreased by just 6% after 10^5 cycles, which is hardly recognizable by human eyes.

In conclusion, we have demonstrated the feasibility of a seamless foldable AMOLED display by showing mechanical and optical tolerances of the folding structure composed of hyperelastic silicone rubber. The optimized design of the folding structure through FEM analysis with ABAQUS resulted in a negligible deterioration of the relative brightness at the junction of the individual panels up to 10^5 cycles of folding-unfolding at a folding radius of 1 mm. These results suggest that the folding structure composed of the commercially available hyperelastic silicon rubber can be applied to mass produce foldable displays, with potentially important technical implications on fabricating large size flexible displays.

[1]D. U. Jin, T. W. Kim, H. W. Koo, D. Stryakhilev, H. S. Kim, S. J. Seo, M. J. Kim, H. K. Min, H. K. Chung, and S. S. Kim, SID Int. Symp. Digest Tech. Papers **41**, 703 (2010).
[2]Y. Kaneko, M. Yamaguchi, H. Matsuya, and T. Tsukada, IEEE Trans. Consum. Electron. **42**, 17 (1996).
[3]M. Aston, J. Soc. Inf. Disp. **15**, 535 (2007).
[4]H. S. Shim, I. S. Kee, Y. G. Lee, I. H. Ko, J. M. Kim, and S. J. Byun, SID Int. Symp. Digest Tech. Papers **39**, 518 (2008).
[5]N. S. Lee, H. S. Shin, H. J. Lee, K. S. Seong, and W. S. Choi, SID Int. Symp. Digest Tech. Papers **33**, 546 (2002).
[6]Y. L. Park, C. Majidi, R. Kramer, P. Berard, and R. J. Wood, J. Micromech. Microeng. **20**, 125029 (2010).
[7]H. J. Kwon, S. W. Lee, and S. S. Lee, Sens. Actuators, A **154**, 238 (2009).
[8]H. J. Kim, C. W. Son, and B. Ziaie, Appl. Phys. Lett. **92**, 011904 (2008).
[9]D. Y. Khang, H. Jiang, Y. Huang, and J. A. Rogers, Science **311**, 208 (2006).
[10]H. S. Shim, I. S. Kee, S. K. Kim, Y. T. Chun, H. J. Kwon, Y. W. Jin, S. Y. Lee, D. W. Han, J. H. Kwack, D. H. Kang, H. K. Seo, M. S. Song, M. H. Lee, and S. C. Kim, SID Int. Symp. Digest Tech. Papers **41**, 257 (2010).
[11]L. Mullins, Rubber Chem. Technol. **42**, 339 (1969).